ASEAN
Journal of Scientific and Technological Reports
Online ISSN: 2773-8752

Research article

Fabrication, 'Optimisation,' Characterization, and *In Vivo* Pharmacokinetic Evaluation of Testosterone Undecanoate Loaded Proniosome Capsule for Enhanced Oral Bioavailability

Ajay Singh[1], Abhishek Soni[2*], and Chinu Kumari[3]

[1] Research Scholar, School of Pharmacy, Abhilashi University, Chail-Chowk, Mandi (H.P.) – 175028, India; saikiamed1@gmail.com
[2] School of Pharmacy, Abhilashi University, Chail-Chowk, Mandi (H.P.) – 175028, India; asoniphd2023@gmail.com
[3] School of Pharmacy, Abhilashi University, Chail-Chowk, Mandi (H.P.) – 175028, India; btpharma2011@gmail.com
* Correspondence: asoniphd2023@gmail.com; (Dr. A. Soni)

Citation:
Singh, A.; Soni, A., Kumari, C. Fabrication-Optimisation, Characterization, and *In Vivo* Pharmacokinetic Evaluation of Proniosome Capsule Loaded with Testosterone Undecanoate for Enhanced Oral Bioavailability. *ASEAN J. Sci. Tech. Report.* **2024**, *27*(3), e250993. https://doi.org/10.55164/ajstr.v27i3.250993

Article history:
Received: September 21, 2023
Revised: March 23, 2024
Accepted: March 27, 2024
Available online: April 20, 2024

Abstract: This study focuses on creating and evaluating proniosome capsules as a potential drug delivery method to increase the oral bioavailability of testosterone undecanoate. The three main stages of the study are proniosome capsule fabrication optimization, characterization, and *in vivo* pharmacokinetic evaluation. The most prominent response surface approach (CCD – Central Composite Design) was used in the fabrication-optimization phase to determine the appropriate ratios of the factors that have the greatest effects on the particle size, PDI, and percentage of drug entrapment of testosterone undecanoate proniosomes. Creating testosterone undecanoate-loaded proniosomal formulations was possible using various ratios of span 60 and cholesterol. The physical and chemical characteristics of proniosome capsules, such as size, shape, surface charge, and drug-release kinetics, such as percentage drug entrapment, Vesicle size (nm), and PDI, must be thoroughly analyzed. Animal models were used to determine how the proniosome capsules affect the bioavailability of testosterone undecanoate after oral administration. Factors like absorption, distribution, metabolism, and excretion are carefully evaluated to determine whether the capsules successfully enhance drug delivery. The reduced particle size, polydispersity index (PDI, 282.33 ± 1.52 nm and 0.181 ± 0.003), and the highest entrapment efficiency (98.12 ± 1.03%) made the optimized formulation the ideal formulation. The Higuchi model provided the most comprehensive justification for releasing the testosterone undecanoate from proniosome compositions. Up to six months of storage, no changes of any type, even those to the proniosomes' color, were seen. There was no drug leakage during the stability study, according to the percentage of drug entrapment data. Positive findings from the *in vivo* pharmacokinetic investigation also suggested that testosterone undecanoate proniosome formulations may last significantly longer than a pure drug in *vivo*.

Keywords: Testosterone undecanoate; proniosome; testosterone insufficiency; vesicular drug delivery; formulation optimization

1. Introduction

To achieve targeted and controlled drug delivery, new drug delivery systems have emerged that incorporate multiple administration routes. One such system that contributes to extending the duration of a drug in systemic circulation and reducing toxicity through selective uptake is drug encapsulation in vesicles. This method has led to the developing of several vesicular drug delivery systems, including liposomes, niosomes, and provesicular systems like proliposomes and proniosomes [1]. Even though the oral route of drug administration has advantages, researchers are constantly looking for newer approaches because they are aware of the major roles that poor drug solubility and absorption, rapid metabolism, high fluctuations in drug plasma, and variability due to food effect play in disappointing *in vivo* results that ultimately cause the conventional delivery system to fail [2, 3].

Due to many new chemical entities (NCEs) and poor water solubility, which impairs therapeutic absorption, effective drug administration is essential [1, 3, 5]. Low solubility, enzyme breakdown, and acidic stomach conditions are among the difficulties associated with oral delivery [2, 3]. Colloidal lipid carriers have been used as treatment, improving drug solubility and gastrointestinal barrier permeability [4-6]. Designing proniosome-like vesicular drug delivery devices shows potential [1, 2]. Due to its limited solubility and promise for increased oral administration, extended-release, and improved patient compliance, testosterone undecanoate was chosen for proniosome manufacture. However, extensive study, formulation improvement, and strict evaluation methods are required to guarantee success.

Age-related increases in testosterone insufficiency prevalence are well-documented, but declining testosterone levels in aging individuals can be partly attributed to illness or senility [7-11]. Symptoms associated with aging and hypogonadism overlap, suggesting a potential link between age-related symptoms and androgen deficiency. However, diagnosing hypogonadism in older males is challenging due to symptom similarities [10, 12, 13]. The conventional testosterone formulation has low oral bioavailability (3-10%) due to hepatic metabolism and poor solubility. Enhancing tablet bioavailability can be achieved through vesicular systems and proniosomes, with potential benefits for oral delivery [12].

Therefore, this current study aimed to determine whether the proniosome could improve the oral bioavailability of testosterone undecanoate despite its poor water solubility and bioavailability. Proniosomes have been established to deliver a wide variety of drugs through the oral route and have been well-known for improving the oral bioavailability of several pharmaceuticals with poor bioavailability. Along with increasing their bioavailability, decreasing first-pass metabolism, lowering their dosage, preventing off-target distribution, preventing an undesired plasma peak, increasing the duration of action, modulating and controlling drug release, and improving the benefit-to-risk ratio, the current study also sought to explore the potential of testosterone undecanoate loaded proniosomes.

2. Materials and Methods

2.1 Material

Testosterone undecanoate and Span 60 were purchased from Sisco Research Laboratories Pvt. Ltd., Mumbai, India. Tween 80 and Span 40 were procured from Thomas Baker (Chemicals) Pvt. Ltd., Mumbai, India. Tween 20 and Cholesterol were purchased from Qualikems Lifesciences Pvt. Ltd., Sadar Bazaar, Delhi, India. Methanol, Potassium Dihydrogen orthophosphate, Sodium hydroxide, and other excipients were procured from Finar, Ahmedabad, Gujarat, India. All other reagents, chemicals, and excipients were of standard pharmaceutical & analytical grade.

2.2 Methods

2.2.1 Drug and excipients compatibility study

The drug and excipients compatibility study is essential to assess chemical and physical interactions between the drug and excipients, ensuring safety and stability and further optimizing the formulation for enhanced efficacy, shelf life, and patient compliance [14, 15].

2.2.1.1 FTIR spectroscopy

FTIR analyses of testosterone undecanoate, Span 60, cholesterol, a physical mixture of testosterone undecanoate, Span 60, cholesterol, mannitol, and optimized proniosome powder were conducted using this method [15, 16].

2.2.1.2 Differential scanning calorimetry (DSC)

The physicochemical composition of the drug in the optimized proniosome formulation was evaluated using DSC analysis. All samples were subjected to a 30 ml/min nitrogen purge while being scanned at 20°C/min from 30 to 350°C [17, 18].

2.2.2 Preparation of the testosterone undecanoate loaded proniosomes (TU-PNs)

Proniosomes loaded with testosterone undecanoate were created using testosterone undecanoate (40 mg) and Span 60/cholesterol at various molar ratios. A slurry technique was used to dissolve the drug and lipid mixtures in 20 ml of a solvent mixture that contained a 2:1 mixture of chloroform and methanol. The resulting mixture was then put into a 100 ml round-bottomed flask with a determined amount of solid carrier and vortexes for 5–10 minutes to create a slurry. The flask was equipped with a rotary evaporator, which was used to evaporate the chloroform and methanol solution for 15-20 minutes at 60°C under decreased pressure. After that, a mortar was used to ground the solid film into powder, and a 100-mesh screen was used to sift it. The obtained proniosome power was vacuum-sealed and kept at room temperature away from light for further evaluation [15, 17, 18].

2.2.3 Screening of the process parameters for preparation of TU-PNs using the slurry method

A variety of process and formulation characteristics were examined to find the optimal conditions for preparing the TU-PNs with the intended outcomes. Effect of different types of surfactant, type of solid carrier, surfactant: cholesterol molar ratio, various amounts of the total lipid, and other amounts of the solid carrier on the appearance, yield, drug entrapment, particle size, PDI, and micrometric properties was evaluated previously in our lab to select the best possible combinations for the fabrication of proniosomes.

2.2.4 Optimization of the TU-PNs using the central composite design

To optimize testosterone undecanoate proniosomes, the study used Central Composite Design (CCD) as the main response surface methodology. The best model among the linear, two-factor interaction and quadratic models was selected using the ANOVA F-value, allowing the development of a second-order polynomial equation to forecast responses [19]. The primary composite design specifications and formulation details were presented in the supplemental material. Design-Expert software made statistical analysis and graph plotting easier. The influence of independent factors on the responses was estimated using Fisher's test and ANOVA. A *P*-value of 0.05 or less was considered statistically significant [19, 20].

2.2.5 In-vitro characterization

2.2.5.1 Percentage yield

Using the following calculation the percent yield of all manufactured TU-PNs was calculated using the below formula [21]:

$$\text{Percentage yield} = \frac{\text{Practical yield}}{\text{Theoretical yield}} \times 100 \quad (1)$$

2.2.5.2 Percentage drug entrapment and Percentage drug loading

Through centrifuging the amount of unentrapped drug (a drug not contained in TU-loaded proniosomes), the encapsulation efficiency (EE) of TU-loaded Proniosomes was measured. Proniosome powder was hydrated with 10 ml of water and vortexed for 5 minutes to create the noisome solution. Around 2 ml of a diluted suspension in an Eppendorf tube was spun at 15000 rpm for 15 minutes at 5oC in a cooling centrifuge to separate the non-encapsulated drug from the suspension. Methanol was used to dilute the supernatant after it had been appropriately removed. By using UV spectroscopy, the amount of free drug was calculated. When calculating the amount of drug that was entrapped, the total amount of drug in the suspension was subtracted from the amount of drug that was not trapped. The following equation calculated the entrapment efficiency and drug loading [22, 23].

$$\text{Entrapment efficiency } (\%) = \frac{\text{Amount of drug present in proniosomes}}{\text{Initial amount of drug added}} \times 100 \quad (2)$$

$$\text{Drug loading } (\%) = \frac{\text{Amount of drug present in proniosomes}}{\text{Amount of drug}-\text{loaded proniosomes}} \times 100 \quad (3)$$

Three different batches of each sample were utilized. Before analysis, TU-PN samples were adequately diluted in a 1:50 ratio with HPLC-grade water. The average of three observations was used to determine the particle size.

2.2.5.3 Micromeritic property

The prepared proniosome formulation's flow properties were measured using various factors like the angle of repose, bulk density, tapped density, Carr's Index, and Hausner's ratio. These were measured by using standard procedures [24].

2.2.5.4 Transmission electron microscopy

Testosterone undecanoate-loaded optimized proniosome formulation morphology and shape were investigated using transmission electron microscopy (TEM, JEM CX 100) [25, 26].

2.2.5.5 In-vitro dissolution

Studies on drug dissolution were performed using pure drugs free of cholesterol and span 60, as well as optimized testosterone undecanoate proniosome formulation. The tests were conducted at 37.0±0.5°C with 900 ml of dissolution medium (pH 1.2 HCl or 6.8 phosphate buffer saline). The apparatus received the equivalent of 40mg of testosterone undecanoate. At set intervals (5, 10, 20, 30, 60, 120, 240, and 300 minutes), samples were removed, replaced with an equivalent new medium, and filtered through a 0.45 membrane. UV spectrophotometers were used at 242 nm [2, 18] to assess the concentrations.

2.2.5.6 In-vitro drug release study

Using the dialysis bag method in sink settings, the release behavior of reconstituted niosome suspension from various formulations and testosterone undecanoate suspension was examined. For 24 hours before usage, the dialysis bags with a cut-off of 8000–14000 kDa were submerged in the 1% ethanolic solution. The proniosome and pure drug equivalent to 40 mg of testosterone undecanoate was accurately measured and poured into the appropriate medium before being poured into the dialysis bag with the two ends snugly sealed and bound on the shaft. Next, 900 ml of release medium (pH 1.2 HCl and pH 6.8 phosphate buffer saline) held at a constant 37.0±0.5^{o}C were added to the dialysis bag. At a rate of 100 revolutions per minute, the paddles were turning. 5ml aliquots were removed and replaced with an equivalent dissolving medium at predetermined time intervals of 0.25 hr, 0.5 hr, 1 hr, 2 hr, 4 hr, 6 hr, 8 hr, 10 hr, 12 hr, 16 hr, and 24 hr. To measure the content of testosterone undecanoate, the withdrawal samples were filtered through a 0.45 membrane filter (0.45 μm Pore Size) and charged into UV spectrophotometers (242 nm) [2, 18].

2.2.5.7 In vitro drug release kinetic study

The release kinetics were analyzed using various kinetic models, including zero-order plots, first-order plots, Higuchi plots, and Korsmeyer Peppas plots [27].

2.2.5.8 Stability analysis

The chosen testosterone undecanoate-loaded proniosome formulation was stored for six months at five °C, 30°C/65%RH, and 40°C/75%RH, respectively, in transparent glass vials. Entrapment effectiveness and drug loading efficiency of proniosome formulations were evaluated every 1, 3, and 6 months compared to newly formed proniosomal [2, 18]. The phase separation and aggregation of all created formulations were visually assessed. Furthermore, significant changes were observed for 6 months. Finally, the estimation of change in physical appearance, percentage of drug entrapment, and percentage of drug loading were evaluated [28].

2.2.6 In vivo pharmacokinetic study

Male Wistar rats weighing 250–300 g were obtained from SBSPM B Pharmacy College, Ambejogai, Beed, India. All animals used in the experiments received care in compliance with the guidelines of The Committee for Control and Supervision of Experiments on Animals. The Institutional Ethical Committee approved the experimental protocol, SBSPM B Pharmacy College, Ambejogai, Beed, India (approval no. CPCSEA – SBSPM/22-23/871). The rats were randomly divided into three groups (n = 3), where group 1 was receiving water *ad libitum* and normal pellet diet only (Control), group 2 was receiving plain pure drug suspension, and group 3 was receiving optimized testosterone undecanoate loaded proniosome formulation, respectively. For the current study, a dose of 10 mg/kg of testosterone undecanoate was employed based on earlier research. Animals were given testosterone proniosomes (100 mg, equivalent to 10 mg of testosterone undecanoate) and a pure drug suspension (10 mg/kg dose) [7, 8, 12]. In compliance with USFDA rules [29], blood samples were taken at predetermined intervals (30 min, 1 hr, 2 hr, 4 hr, 6 hr, 8 hr, 10 hr, 12 hr, and 24 hr), given the drug's 2-hour half-life. Serum was collected by centrifuging blood samples at 3000 rpm for 12

minutes, which was then kept at -20°C for later HPLC analysis [7, 8, 12]. The accurate assessment of the pharmacokinetics of testosterone undecanoate was made possible by this stringent approach. The pharmacokinetic parameters such as mean residence time (MRT), elimination rate constant (k_e), maximum plasma concentration (Cmax), and time to achieve the maximum plasma concentration (T_{max}) were obtained from the plasma concentration versus time curve. The area under the plasma concentration-time curve from time zero to the final concentration time point (AUC0-t) and the area under the plasma concentration-time curve from time zero to infinity (AUC0–∞) was also calculated using the measured drug plasma concentrations. The acquired information was presented as mean standard deviation [30].

2.2.7 Statistical analysis

All the results are the mean ± SD of three independent experiments. The significance of differences ($P < 0.05$) between experimental variables was determined by the use of a two-tailed Student's test as well as by one-way ANOVA (Analysis of Variance) followed by *post hoc* Turkey's test (GraphPad Software Package, Version 8). The statistical significance was indicated by $P < 0.05$.

3. Results and Discussion

3.1 Determination of absorption maxima of testosterone undecanoate

The drug's maximum absorption was determined by using a UV spectrophotometer to scan a 12µg/ml solution of testosterone undecanoate in methanol between 200 and 400 nm. The 242 nm UV absorption maxima were discovered to be relatively near to the absorption maxima reported in the literature [7, 9].

3.2 Drug and excipients compatibility study

The retention of significant peaks, indicating compatibility, was confirmed by the FTIR analysis of testosterone undecanoate, span 60, cholesterol, and mannitol separately and in a physical mixture (figure 1). The absence of any incompatibility ensured stability. A crystal structure with melting peaks at 61.30°C was visible in Span 60. The optimized proniosome formulation showed testosterone undecanoate's endothermic peak at 64.35°C, indicating effective encapsulation inside the proniosomes. This analysis demonstrated the stable integration of drugs and excipients, crucial for the formulation's effectiveness and safety.

3.3 Preparation of the Testosterone undecanoate loaded proniosomes (TU-PNs)

Proniosomes, loaded with testosterone undecanoate and nonionic surfactant span 60, were created using a literature-described technique [15, 18, 30]. Despite the advantages, traditional noisome dispersions face issues like aggregation and drug leakage. The proniosome technique resolves these problems, ensuring stable aqueous niosomes. Tactics like adding cholesterol are employed to enhance vesicle stability in stomach juices. Nonionic surfactant and cholesterol concentrations determine niosome stability; any change leads to drug leakage. Interestingly, the creation of niosomes from proniosome powder occurred spontaneously, forming vesicular structures on the carrier's surface, transforming into spherical multilamellar vesicles with gentle agitation, aligning with existing literature studies [15, 18, 30].

3.4 Optimization of testosterone-loaded proniosome using the central composite design

The central composite design is one of the response surface models used in experiment design to hit the mark, eliminate variability, and maximize or minimize reactions that increase product production or decrease waste. Utilizing the central composite response surface methodology, the ratio of the amounts of span 60 and cholesterol were two of the three significant variables chosen based on the initial Screening results. These variables were used to reduce the particle size and increase the loading efficiency of the testosterone undecanoate proniosome (Table 3).

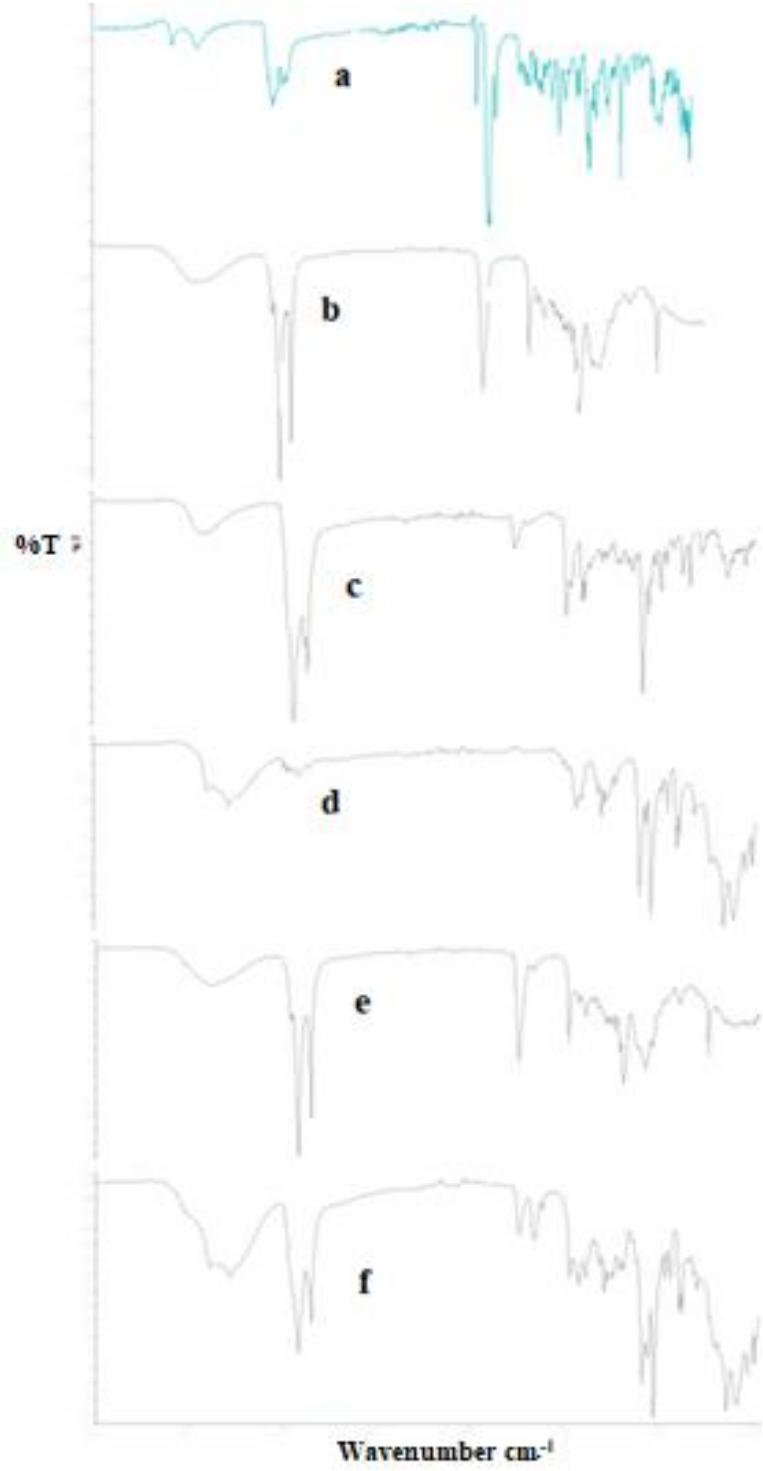

Figure 1. FTIR spectra of the testosterone undecanoate (a), span 60 (b), cholesterol (c), mannitol (d), a physical mixture consisting of testosterone undecanoate, span 60, cholesterol and mannitol (e) and optimized formulation (f, DTU-PNs14)

Table 3. Composition of the testosterone undecanoate proniosome with response

Formulation code	Factor 1 X1: Amount of SPAN 60 (μM)	Factor 2 X2: Amount of cholesterol (μM)	Response Y1 Percentage drug entrapment (%)	Response Y2 Vesicle size (nm)	Response Y3 PDI
DTU-PNs1	160.3553391	125	99.61	335.05	0.238
DTU-PNs2	100	100	80.00	279.14	0.220
DTU-PNs3	125	89.64466094	84.68	258.29	0.214
DTU-PNs4	125	125	97.84	283.00	0.181
DTU-PNs5	125	160.3553391	90.69	281.02	0.218
DTU-PNs6	89.64466094	125	85.69	300.08	0.235
DTU-PNs7	125	125	98.85	284.15	0.178
DTU-PNs8	125	125	98.71	286.27	0.180
DTU-PNs9	100	150	90.17	284.32	0.230
DTU-PNs10	125	125	98.54	285.18	0.179
DTU-PNs11	150	150	94.17	319.20	0.226
DTU-PNs12	150	100	95.78	293.12	0.228
DTU-PNs13	125	125	97.91	285.08	0.177

All the formulations' results were evaluated to determine the best study design. Software called Design Expert 7.0 was used to create contour plots and a desirability plot. A quadratic model was proposed regarding particle size, PDI, and entrapment effectiveness. ANOVA was used to determine the factors that significantly impacted the replies (Analysis of variance). The findings showed that the chosen independent variables had a significant impact on the chosen answers because the ranges for particle size (nm), PDI, and entrapment efficiency (%) were, respectively, 281-335 nm, 0.178-0.238, and 80.00-99.61%.

3.4.1 Percentage drug entrapment (Y1)

The impact of span 60 and the amount of cholesterol on percentage drug entrapment on particle size was studied, and the responses obtained were given in Tables 4 and 5.

Table 4. Model Summary Statistics

Model	Std. Dev.	R-Squared	Adjusted R-Squared	Predicted R-Squared	PRESS	
Linear	5.2034	0.4605	0.3526	0.0777	462.8394	
2FI	5.1214	0.5296	0.3728	-0.0542	529.0455	
Quadratic	0.3599	0.9982	0.9969	0.9967	1.6353	Suggested
Cubic	0.4255	0.9982	0.9957	0.9925	3.7753	Aliased

The model's significance, denoted by the large Model F-value of 773.38 (occurring due to noise only 0.01% of the time), highlights the significance of terms X1, X2, X1X2, $X1^2$, and $X2^2$ ('Prob > F' < 0.0500). Model reduction, excluding unnecessary terms (except for hierarchy maintenance), could enhance the model's accuracy. The 'Lack of Fit F-value' of 0.06 indicates insignificance compared to pure error, with a 97.80% probability of being caused by noise. A non-significant lack of fit is desirable for a well-fitting model. The experimental model displayed minimal deviations, evident in high R^2 (0.9981), adjusted R^2 (0.9969), and predicted R^2 (0.9967) values. Predictions for particle size, based on specific element amounts, were made using a polynomial equation in terms of coded factors, ensuring accurate estimations. The equation is as follows:

Percentage drug entrapment (Y1) = 98.37+ 4.933231599 X1+ 2.132427939X2 -2.945 X1X2- 2.894375$X1^2$- 5.376875$X2^2$ (4)

The entrapment efficiency (EE) of testosterone undecanoate was enhanced by elevated cholesterol and span 60 levels. The molecule was more easily accommodated by the higher lipophilic environment produced by lipophilic surfactants with substantial hydrophobic components. These surfactants produced well-closed, uniformly packed bilayer structures. They ordered gel states due to their high transition temperatures (Tc) and low HLB values (4-6), which enabled the highly lipophilic material to be intercalated effectively. Increased entrapment was caused by the surfactant's solid state, hydrophobicity, and high phase transition temperature. However, for other formulae, a rise in TU content resulted in a drop in EE, except for one where a higher surfactant concentration inhibited drug entrapment because excessive surfactant had destabilized lipid bilayers. The 3D response plot shows that this instability caused quick drug diffusion and a decrease in percent EE, possibly leading to the formation of pores.

Cholesterol addition makes the formulation dense, indicating a stiffer bilayer membrane. Furthermore, highly organized surfactant and cholesterol systems allow easier drug partitioning. The structure of the surfactant phase affected the lamellar surfactant phase's capacity to accommodate drugs. The higher stability and bilayer hydrophobicity for niosomes might cause a rise in testosterone undecanoate entrapment efficiency with increased cholesterol content.

Table 5. Entrapment efficiency ANOVA Response for Quadratic Model.

Source	Sum of Squares	df	Mean Square	F Value	p-value Prob > F	
Model	500.9188	5	100.1838	773.3816	< 0.0001	significant
X1-Amount of SPAN 60 (A)	194.6942	1	194.6942	1502.967	< 0.0001	
X2-Amount of cholesterol (B)	36.37799	1	36.37799	280.8247	< 0.0001	
X1X2	34.6921	1	34.6921	267.8102	< 0.0001	
$X1^2$	58.27761	1	58.27761	449.8816	< 0.0001	
$X2^2$	201.1185	1	201.1185	1552.561	< 0.0001	
Residual	0.906779	7	0.12954			
Lack of Fit	0.039379	3	0.013126	0.060532	0.9780	not significant
Pure Error	0.8674	4	0.21685			
Cor Total	501.8256	12				
R-Squared	0.9982					
Adj R-Squared	0.9969					
Pred R-Squared	0.9967					
Adeq Precision	79.626					

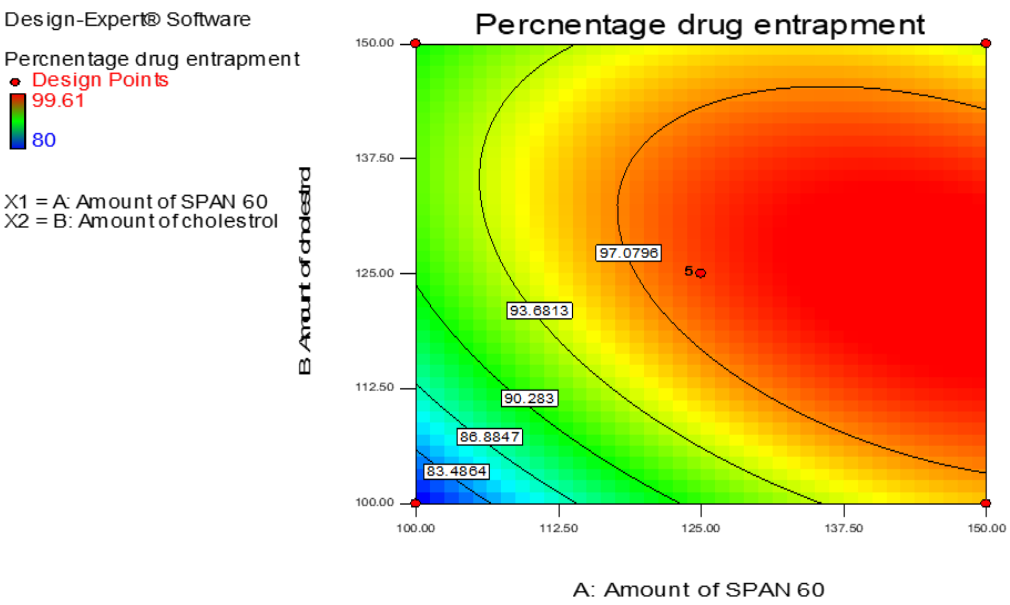

Figure 2. The counterplot of the response

The link between the dependent and independent variables was clarified by creating contour plots. Figure 2 displays the impacts of X1 and X2 together with their interaction on the percentage of drug entrapment. Up to 93% PDE, the graphs were found to be linear, but above this point, the plots were found to be nonlinear, indicating a nonlinear relationship between X1 and X2.

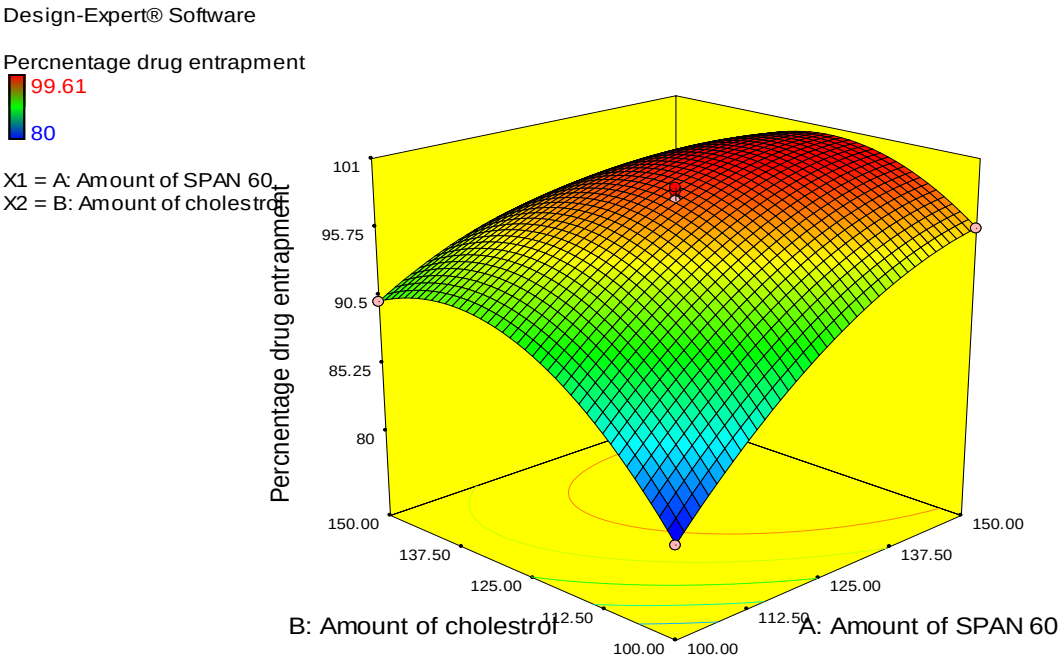

Figure 3. 3D response graph

The effects of independent variables on EE were depicted using 3D response surface plots. It was discovered that all DTU-PNs had EE percentages ranging from 80 to 99.61%. As the concentration of span 60, cholesterol (CHO), and drug increases, so does the EE (%) of testosterone undecanoate. By strengthening the lipid bilayer and reducing drug leakage, cholesterol improved the EE. Additionally, Span 60 concentration

increased the EE of testosterone undecanoate in proniosomes, which increased the maximal phase transition temperature. It was also discovered that all formulae displayed a different degree of EE decrease with an increase in TU content, except for one formulation where a higher concentration of the surfactant reduced the percentage of drug entrapment because a higher concentration of the surfactant might cause the destabilization of lipid bilayers. The following elements may play a role in why entrapment efficiency declines as cholesterol proportions rise above a certain point in time:

(1) The diameter of the bilayer shrank due to the increase in cholesterol, resulting in a smaller interspace;

(2) the increased cholesterol might fight with testosterone undecanoate for packing space within the bilayer. Additionally, the elevated cholesterol might have harmed the bilayer's normal linear shape, leading to the leakage of the entrapped drug, as shown in the 3D response plot (Figure 3).

3.4.2 Vesicle size

According to Table 6, the proniosome formulae's vesicles ranged in size from 279.14 nm to 335.04 nm. Smaller vesicles resulted from the homogeneous thin film of the surfactant mixture being hydrated more effectively with low surfactant amounts than more significant surfactant amounts. The high cholesterol content in the formulation may be the cause of the large size of the cysts. It was claimed that cholesterol made the lipid bilayers wider. Additionally, by lowering the peak temperature at which the vesicle phase transition occurs, it is in charge of increasing the rigidity and strength of the bilayer membrane of the vesicles and decreasing their fluidity [15, 18, 30].

Analysis of variance (ANOVA) was implemented to recognize the significant terms of the quadratic model on vesicle size. Multiple regressions were done to vesicle size values at various levels of the two factors (X1 and X2) to give up a regression equation determination coefficient (R^2) of 0.99.

Table 6. Model Summary Statistics and ANOVA

Model Summary Statistics						
Source	**Std. Dev.**	**R-Squared**	**Adjusted R-Squared**	**Predicted R-Squared**	**PRESS**	
Linear	16.31716	0.391186	0.269423	-0.30585	5710.814	
2FI	16.84338	0.416157	0.221542	-0.29185	5649.603	
Quadratic	0.955611	0.998538	0.997494	0.997251	12.02233	Suggested
Cubic	1.118049	0.998571	0.99657	0.994562	23.77999	Aliased
ANOVA						
Source	**Sum of Squares**	**df**	**Mean Square**	**F Value**	**p-value Prob > F**	
Model	4366.862	5	873.3723	956.3942	< 0.0001	significant
A-Amount of SPAN 60	1208.231	1	1208.231	1323.084	< 0.0001	
B-Amount of cholesterol	502.5254	1	502.5254	550.295	< 0.0001	
AB	109.2025	1	109.2025	119.5832	< 0.0001	
A^2	1893.511	1	1893.511	2073.507	< 0.0001	
B^2	386.8043	1	386.8043	423.5735	< 0.0001	
Residual	6.39235	7	0.913193			
Lack of Fit	0.36663	3	0.12221	0.081126	0.9668	not significant
Pure Error	6.02572	4	1.50643			
Cor Total	4373.254	12				
R-Squared	0.998538308					
Adj R-Squared	0.997494242					
Pred R-Squared	0.997250941					
Adeq Precision	117.8329807					

The model's significance, indicated by the Model F-value of 956.39 (occurring in noise only 0.01% of the time), led to the significance of terms X1, X2, X1X2, $X1^2$, and $X2^2$ ('Prob > F' < 0.0500). Model reduction excluding unnecessary terms maintains hierarchy. The 'Lack of Fit F-value' of 0.11, not significant compared to pure error, suggests good model fit, with R^2 (0.9985), adjusted R^2 (0.9975), and predicted R^2 (0.9973) showing minimal experimental differences. A polynomial equation, derived from coded factors, predicted particle size for specific element amounts:

$$\text{Vesicle size (Y2)} = 284.74 + 12.29\,X1 + 7.93\,X2 + 5.23\,X1X2 + 16.50\,X1^2 - 7.46\,X2^2 \quad (5)$$

Span 60 and cholesterol levels affected the size of testosterone undecanoate vesicles, demonstrating the surfactant's hydrophobicity. Adding Span 60 resulted in more giant vesicles, whereas low surfactant concentrations produced smaller, hydrated vesicles. Cholesterol initially decreased vesicle size and shrank after that [4, 11, 13]. Higher cholesterol was connected with more giant vesicles (>100 nm). However, increased cholesterol levels thickened the bilayer and decreased fluidity, as shown in the 3D response graph. Underscoring the complexity of their interactions, the complicated interplay between surfactant and cholesterol had a major impact on vesicle properties.

The link between the dependent and independent variables was clarified by creating contour plots. The effects of X1 and X2 with their interaction on vesicle size are shown in Figures 4 and 5. The plots were found to be nonlinear, indicating a nonlinear relationship between X1 and X2

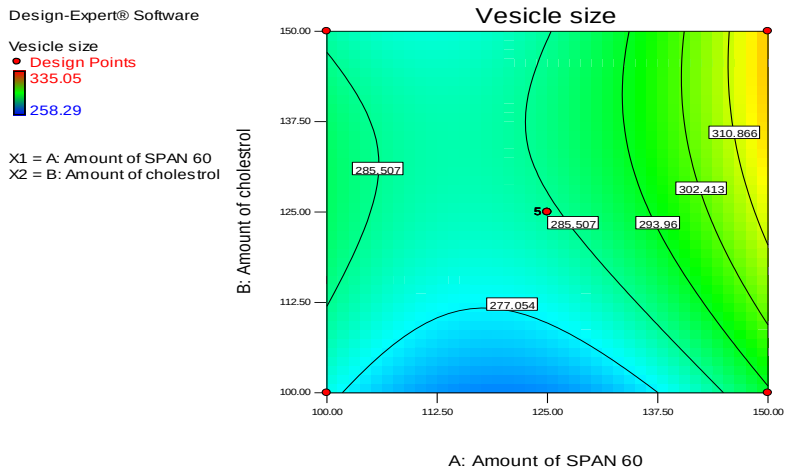

Figure 4. Counter plot

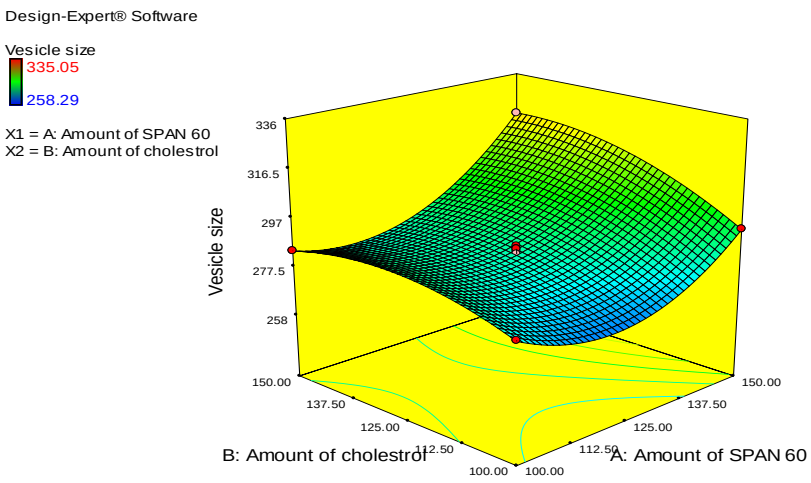

Figure 5. 3D response graph

3.4.3 Polydispersity index (PDI)

The PDI of the proniosome formulae ranged from 0.177 -0.238, as shown in Table 7. Analysis of variance (ANOVA) was implemented to recognize the significant terms of the quadratic model on PDI. Multiple regressions were done to vesicle size values at various levels of the two factors (X1 and X2) to give up a regression equation (Eq. the determination coefficient (R^2) of 0.99.

Table 7. Model Summary Statistics and ANOVA

Model Summary Statistics						
Source	**Std. Dev.**	**R-Squared**	**Adjusted R-Squared**	**Predicted R-Squared**	**PRESS**	
Linear	0.027019	0.004338	-0.19479	-0.6035	0.011757	
2FI	0.02841	0.009248	-0.321	-1.19017	0.016058	
Quadratic	0.001243	0.998524	0.997471	0.997075	2.14E-05	Suggested
Cubic	0.001423	0.998619	0.996686	0.996778	2.36E-05	Aliased
ANOVA						
Source	**Sum of Squares**	**df**	**Mean Square**	**F Value**	**p-value Prob > F**	
Model	0.007321	5	0.001464	947.4059	< 0.0001	significant
A-Amount of SPAN 60	8.49E-06	1	8.49E-06	5.495	0.0515	
B-Amount of cholesterol	2.33E-05	1	2.33E-05	15.08469	0.0060	
AB	3.6E-0	1	3.6E-05	23.29311	0.0019	
A^2	0.005725	1	0.005725	3704.269	< 0.0001	
B^2	0.002365	1	0.002365	1530.105	< 0.0001	
Residual	1.08E-05	7	1.55E-06			
Lack of Fit	8.19E-07	3	2.73E-07	0.109153	0.9503	not significant
Pure Error	0.00001	4	2.5E-06			
Cor Total	0.007332	12				
R-Squared	0.9985					
Adj R-Squared	0.9975					
Pred R-Squared	0.9971					

The model's significance, indicated by the large Model F-value of 947.4059 (occurring due to noise only 0.01% of the time), highlights the significance of terms X1, X2, X1X2, $X1^2$, and $X2^2$ ('Prob > F' < 0.0500). Model reduction, excluding unnecessary terms except for hierarchy-maintaining ones, could enhance the model's accuracy. The 'Lack of Fit F-value' of 0.11 indicates minor significance compared to pure error, primarily caused by noise (95.03%). A minimal lack of fit is desirable for a well-fitting model. The experimental model displayed minimal fluctuations, evident in high R^2 (0.9985), adjusted R^2 (0.9975), and predicted R^2 (0.9971) values. Predictions for particle size, based on specific factor levels, were made using a polynomial equation in coded factors, ensuring accurate estimations. The equation is as follows:

$$PDI\ (Y3) = 0.18 + 1.03\ X1 + 1.07X2 - 3.00\ X1X2 + 0.029X1^2 - 0.018X2^2 \quad (6)$$

The positive coefficients of X1 show that span 60 increases with a rise in vesicles PDI. Here, the surfactant (span 60, X1) has a favorable impact on PDI, increasing PDI for PNs as the concentration of span60 is raised. Cholesterol has a biphasic impact on PDI. The effect of cholesterol and amount of span 60 on the PDI of PNs was shown in the 3D response graph.

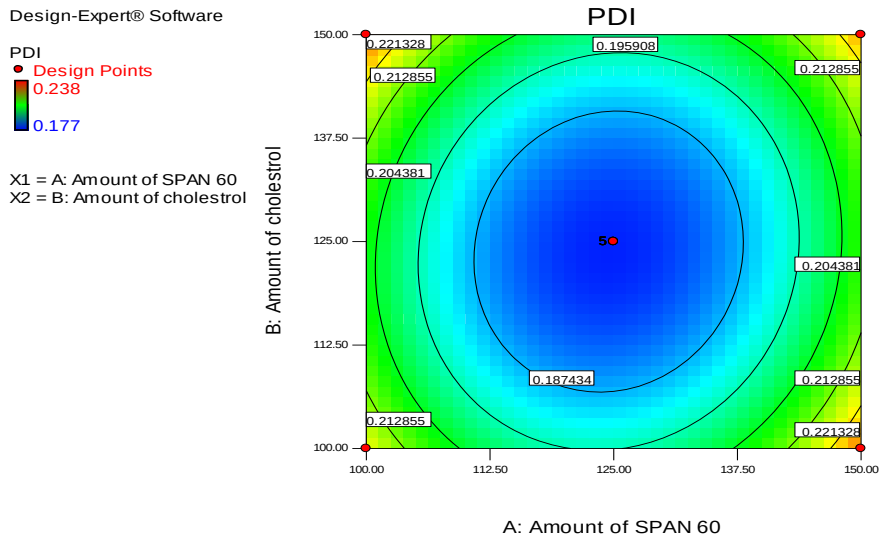

Figure 6. Counter plot

The relationship between the dependent and independent variables was further elucidated by constructing contour plots. The effects of X1 and X2 with their interaction on PDI are shown in Figure 7. The plots were nonlinear, indicating a nonlinear relationship between X1 and X2.

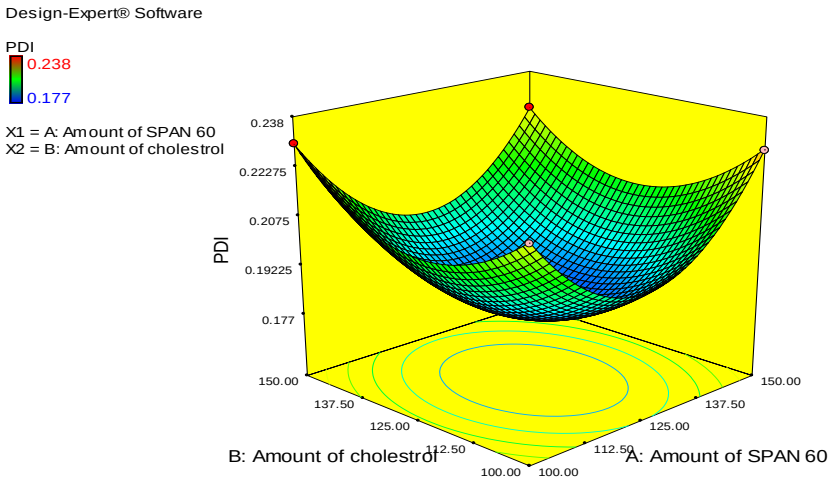

Figure 7. 3D response graph.

3.4.4 Checkpoint analysis

Expected mean vesicle diameter (MVD) and percentage drug entrapment (PDE) values were validated during the fabrication and evaluation of a checkpoint batch, validating the predictive accuracy of the derived coefficients and contour plots. In terms of drug entrapment, vesicle size, and PDI, standard deviation comparisons between actual and predicted values did not find any appreciable variations. The best formulation, DTU-PNs14, was chosen due to the study's determination of the coefficients' accuracy in predicting the values of independent variables. This formulation ensures small vesicle size, low PDI, and maximum entrapment efficiency. Therefore, formulation DTU-PNs14 was deemed to be the most optimal formulation since it had the lowest particle size and PDI (282.33 ± 1.52 nm and 0.181 ± 0.003) and the highest entrapment efficiency (98.12 ± 1.03%).

Table 8. Composition of the optimized formulation with the predicted and actual value of the percentage drug entrapment, vesicle size, and PDI

Predicted						
Formulation code	**Amount of SPAN 60 (μM)**	**Amount of cholesterol (μM)**	**Percentage drug entrapment (%)**	**Vesicle size (nm)**	**PDI**	**Desirability**
DTU-PNs14	125.36	123.09	98.249	284.261	0.179	0.841
Actual						
Formulation code	**Percentage drug entrapment (%)**		**Vesicle size (nm)**		**PDI**	
DTU-PNs14	98.12 ± 1.03		282.33 ± 1.52		0.181 ± 0.003	

3.5 *In vitro* characterization parameters

3.5.1 Percentage yield, Percentage drug entrapment, Percentage drug loading, Vesicle size and PDI

The percentage yield of all prepared formulations is shown in Table 9. The percentage yield of all prepared formulations was determined to be between 98.24 ± 0.65% to 99.64 ± 0.53%. The optimized formulation DTU- PNs14's percentage yield was discovered to be 99.41 ± 0.20%. The range of the testosterone undecanoate drug entrapment percentage in the entire formulation was determined to be between 80.00 ± 0.10% and 99.61 ± 0.03%. Whereas the percentage of drug entrapment of the optimized formulation DTU-PNs14 was 98.12 ± 0.03%. It was discovered that the percentage drug loading of all produced formulations ranged from 8.16 ± 0.01 to 10.16 ± 0.06. While the optimized formulation DTU-PNs14 drug loading was discovered to be 10.06 ± 0.01%. Vesicle size and PDI of all created formulations were determined to be between 258.29 ± 1.63nm to 335.05 ± 1.01 and 0.177 ± 0.004 to 0.238 ± 0.002, respectively. While the optimized formulation DTU-particle PNs14's size and PDI were discovered to be 282.33 ± 1.52nm and 0.181 ± 0.003, respectively.

Table 9. Percentage yield, Percentage drug entrapment, Percentage drug loading, Vesicle size, and PDI of all prepared formulations.

Formulation code	**Percentage yield (%)**	**% Drug entrapment**	**Percentage drug loading**	**Vesicle size (nm)**	**PDI**
DTU-PNs1	98.88 ± 0.66	99.61 ± 0.03	10.16 ± 0.06	335.05 ± 1.01	0.238 ± 0.002
DTU-PNs2	98.24 ± 0.65	80.00 ± 0.10	8.16 ± 0.01	279.14 ± 0.99	0.220 ± 0.003
DTU-PNs3	99.42 ± 0.48	84.68 ± 0.26	8.64 ± 0.04	258.29 ± 1.63	0.214 ± 0.004
DTU-PNs4	98.33 ± 0.39	97.84 ± 0.05	9.98 ± 0.01	283.00 ± 1.00	0.181 ± 0.002
DTU-PNs5	99.06 ± 0.54	90.69 ± 0.30	9.26 ± 0.03	281.02 ± 1.42	0.218 ± 0.004
DTU-PNs6	99.18 ± 0.55	85.69 ± 0.02	8.74 ± 0.02	300.08 ± 1.05	0.235 ± 0.003
DTU-PNs7	99.44 ± 0.27	98.85 ± 0.05	10.09 ± 0.04	284.15 ± 1.82	0.178 ± 0.003
DTU-PNs8	99.22 ± 0.52	98.71 ± 0.08	10.07 ± 0.02	286.27 ± 0.84	0.180 ± 0.006
DTU-PNs9	99.52 ± 0.51	90.17 ± 0.30	9.13 ± 0.05	284.32 ± 0.94	0.230 ± 0.004
DTU-PNs10	99.39 ± 0.63	98.54 ± 0.04	10.00 ± 0.03	285.18 ± 1.20	0.179 ± 0.003
DTU-PNs11	99.01 ± 0.67	94.17 ± 0.67	9.59 ± 0.07	319.20 ± 1.98	0.226 ± 0.005
DTU-PNs12	99.64 ± 0.53	95.78 ± 0.69	9.77 ± 0.02	293.12 ± 0.94	0.228 ± 0.008
DTU-PNs13	99.03 ± 0.42	97.91 ± 0.11	10.04 ± 0.01	285.08 ± 1.80	0.177 ± 0.004
DTU-PNs14	99.41 ± 0.20	98.12 ± 0.03	10.06 ± 0.01	282.33 ± 1.52	0.181 ± 0.003

3.5.2 Micromeritic properties

Micromeritic properties of all prepared testosterone undecanoate-loaded proniosome formulations are shown in Table 10. All prepared formulations' Micromeritic parameters, such as the bulk density, tapped density, Carr's index, and Hausner ratio, were found to fall within the following ranges: 0.157 ± 0.002 to 0.218 ± 0.001, 0.167 ± 0.001 to 0.226 ± 0.001, 1.538 ± 0.377 -9.221 ± 1.742%, 1.016 ± .0004-1.102 ± 0.021. The values of the bulk

density tapped density, Carr's index, and Hausner ratio for the optimized formulations were determined to be 0.218 ± 0.001g/cm^3, 0.226 ± 0.001 g/cm^3, 3.583 ± 0.426%, and1.037 ± 0.005, respectively.

Table 10. Micromeritic properties of all prepared testosterone undecanoate proniosome formulations, including the optimized formulation

Formulation code	Bulk density (gm/cm^3)	Tapped density (gm/cm^3)	Carr's index (%)	Hausner ratio
DTU-PNs1	0.160 ± 0.002	0.167 ± 0.001	3.912 ± 1.302	1.041 ± 0.014
DTU-PNs2	0.164 ± 0.001	0.174 ± 0.001	5.826 ± 0.804	1.062 ± 0.009
DTU-PNs3	0.186 ± 0.002	0.200 ± 0.001	7.016 ± 1.220	1.076 ± 0.014
DTU-PNs4	0.212 ± 0.002	0.222 ± 0.001	4.236 ± 1.369	1.044 ± 0.015
DTU-PNs5	0.157 ± 0.002	0.173 ± 0.022	9.221 ± 1.742	1.102 ± 0.021
DTU-PNs6	0.171 ± 0.001	0.181 ± 0.002	5.693 ± 1.920	1.061 ± 0.022
DTU-PNs7	0.208 ± 0.003	0.216 ± 0.003	3.699 ± 1.433	1.039 ± 0.015
DTU-PNs8	0.200 ± 0.002	0.213 ± 0.002	5.774 ± 1.837	1.062 ± 0.021
DTU-PNs9	0.188 ± 0.001	0.197 ± 0.002	4.785 ± 1.265	1.050 ± 0.014
DTU-PNs10	0.198 ± 0.002	0.201 ± 0.001	1.538 ± 0.377	1.016 ±. 0004
DTU-PNs11	0.165 ± 0.002	0.177 ± 0.003	6.948 ± 1.703	1.075 ± 0.019
DTU-PNs12	0.192 ± 0.001	0.203 ± 0.003	5.541 ± 1.309	1.059 ± 0.015
DTU-PNs13	0.201 ± 0.002	0.215 ± 0.002	6.466 ± 1.504	1.069 ± 0.007
DTU-PNs14	0.218 ± 0.001	0.226 ± 0.001	3.583 ± 0.426	1.037 ± 0.005

3.5.3 Transmission electron microscopy

Vesicle formation on further dilution of the optimized formulation proniosome powder with water was further confirmed by TEM, as shown in Figure 8.

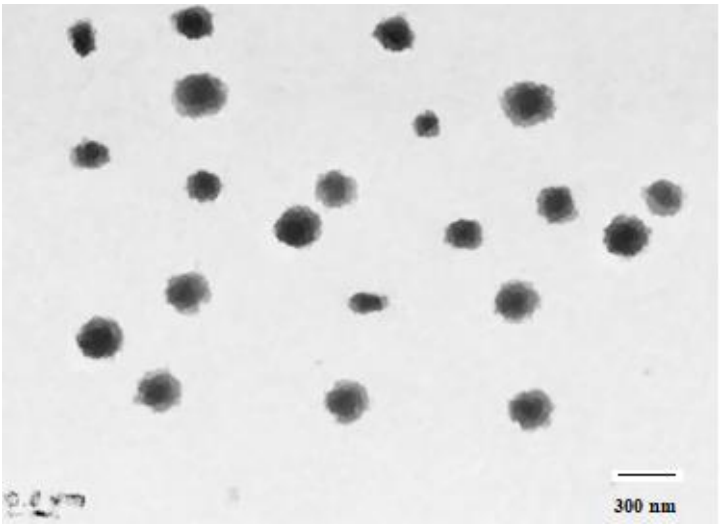

Figure 8. TEM image of the optimized formulation of the DTU-PNs14 Upon dilution of the proniosome powder with the water

The niosome was an easily recognized, nearly perfect sphere with an internal aqueous space, as shown in Figure 8. Additionally, the outermost bilayer could be seen. Additionally, the proniosome vesicle had a spherical shape, and no signs of drug crystal or aggregation were found. It could be quickly redistributed in water.

3.5.4 In vitro dissolution study

The dissolution profile of pure drug and TU-loaded proniosome powder in HCl (pH 1.2) and phosphate buffer solution (pH 6.8) is shown in Figure 9.

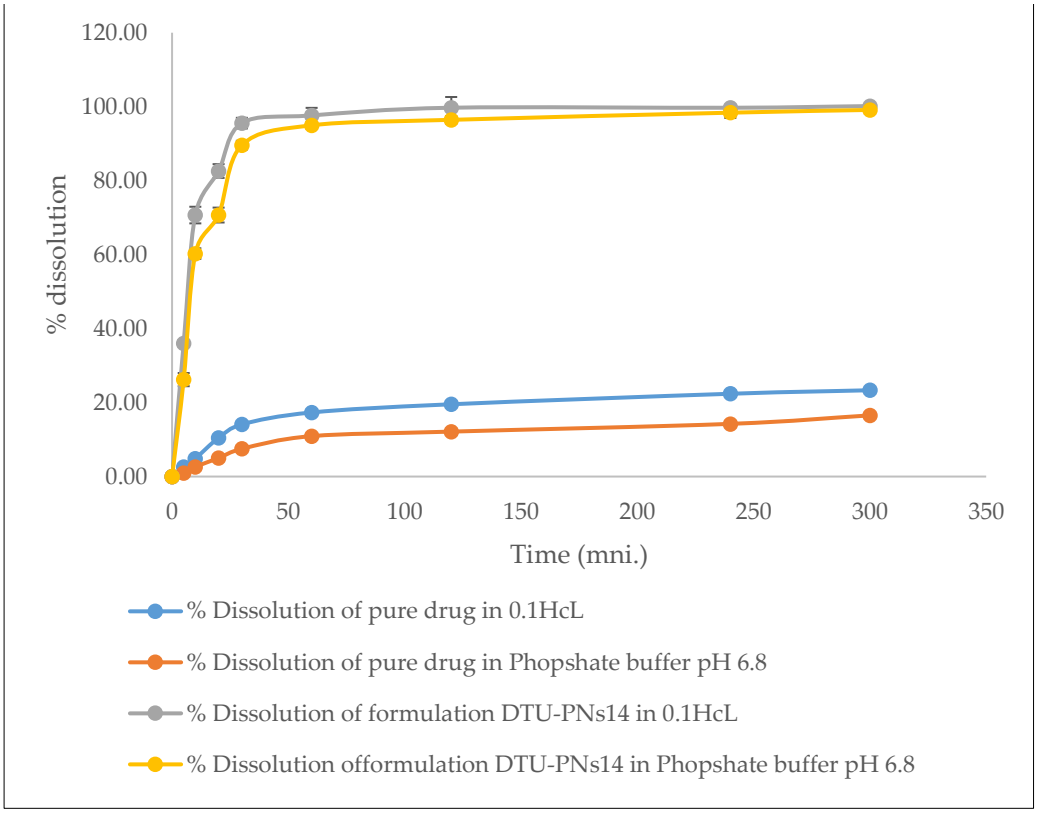

Figure 9. Comparison of the *in-vitro* dissolution profile of the pure drug and TU-loaded proniosome powder in different media

It was evident that testosterone undecanoate dissolved much more quickly in HCl (pH 1.2) than in phosphate buffer solution (pH 6.8). In contrast to the 7–14% of testosterone undecanoate from the pure drug, after 30 min., the dissolving amount of testosterone undecanoate from proniosome was above 89–95% in both buffer HCl (pH 1.2) and phosphate buffer solution (pH 6.8). This might be because of the increased solubility of testosterone undecanoate in proniosomes. This was presumably caused by the fact that testosterone undecanoate was distributed in the proniosome powder in a molecular or amorphous state and that the large surface area of the proniosome powder boosted the drug's drug dissolution rate, causing faster dissolution.

3.5.5 In vitro drug release study

Figure 10 illustrates testosterone undecanoate releases from proniosome formulations and testosterone undecanoate pure drug suspension.

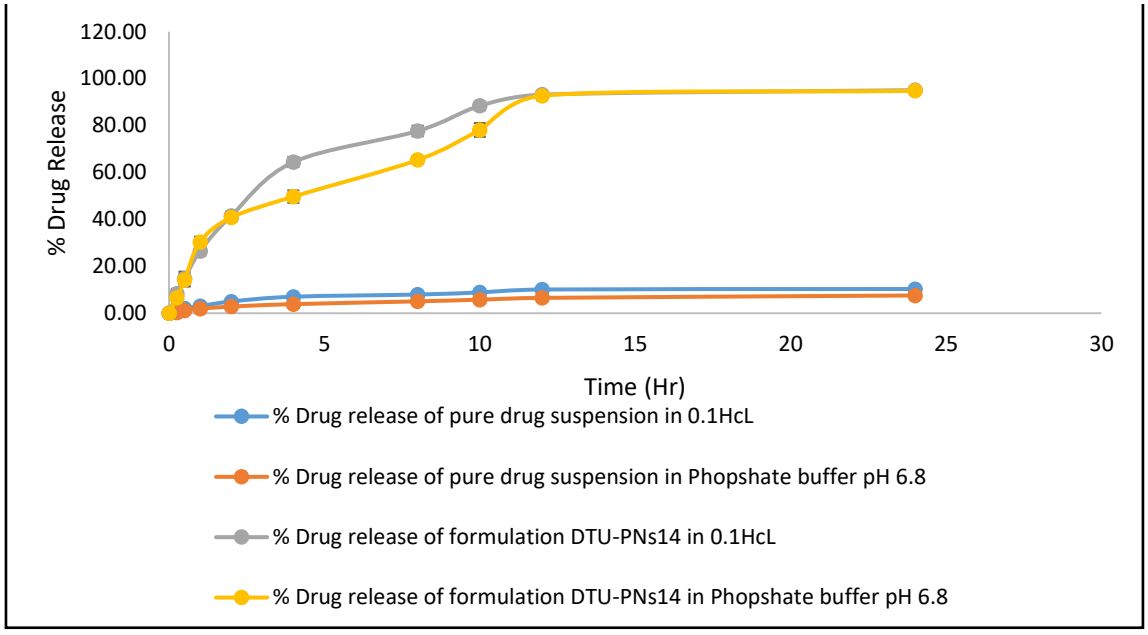

Figure 10. Comparison of the in vitro drug release profile of the testosterone undecanoate from pure drug suspension and TU-loaded proniosome powder in different media

Proniosome formulation had a much higher release rate in phosphate buffer solution (pH 0.1 or 6.8) than testosterone undecanoate pure drug suspension. In contrast to the testosterone undecanoate 26.50 ± 2.01% and 30.37 ± 2.25% from the proniosome formulation, only 3.01 ± 0.25% and 1.91 ± 0.09% of the drug from the testosterone undecanoate pure drug suspension was released in pH 1.2 and 6.8pH, respectively. A clear concentration gradient between the niosomes and the medium was thought to form as the non-trapped drug was released, causing a more rapid release than pure drug suspension. Additionally, after 24 hours, testosterone undecanoate pure drug suspension released 10.31 ± 0.18% and 7.56 ± 0.22% of the drug, whereas proniosome formulation released 95.10 ± 0.86% and 94.81 ± 1.57% of the drug. This was probably because testosterone undecanoate was incorporated into Niosomes, which protected the drug from environmental conditions. From these results, we can conclude that niosomes contributed to the differences between the release of testosterone undecanoate from the proniosome formulations and testosterone undecanoate pure drug suspension.

3.5.6 Percentage drug release kinetic study

Percentage drug release kinetics parameters of the release of the testosterone undecanoate from the optimized proniosome formulations DTU-PNs14 in 0.1N Hcl and pH 6.8 phosphate buffer are as follows:

Table 11. Drug release kinetic model of the optimized formulation DTU-PNs14 in 0.1NHcl and pH 6.8 phosphate buffer

S. No.	Name of media	Regression coefficient			
		Zero-order	First order	Higuchi order	Korsmeyer peppas
1	0.1NHcl	0.698	0.881	0.912	0.541
2	pH 6.8 phosphate buffer	0.765	0.901	0.942	0.553

Table 11 confirms that the testosterone undecanoate release from the proniosomes formulations was best explained by the Higuchi model because it has a higher regression coefficient value than the other models.

3.5.7 Stability study

At predetermined intervals of 1 month, three months, and six months, the proniosomal formulations were assessed for their physical appearance, percentage of drug entrapment, and percentage of drug loading. The stability study of the optimized testosterone undecanoate loaded proniosome formulations was carried out at three different storage conditions, namely 5°C, 30°C/65%RH, and 40°C/75%RH for 6 months. The results

revealed that no changes were noticed under various storage conditions over different time intervals (Table 12). It was observed that there was no change in the color of the proniosomes up to 6 months of storage. The results of the percentage drug entrapment indicated no leakage of the drug.

Table 12. Stability study of DTU-PNs14 indicating physical appearance, percentage drug entrapment, and percentage drug loading

Month	Physical appearance	Percentage drug entrapment			Percentage drug loading		
		Storage condition			Storage condition		
		5°C	30°C/65%RH	40°C/75%RH	5°C	30°C/65%RH	40°C/75%RH
0	White free flowing powder	98.12 ± 0.03	98.12 ± 0.030	98.12 ± 0.030	10.06 ± 0.01	10.05 ± 0.01	10.05 ± 0.01
1	White, free-flowing powder	98.04 ± 0.05	97.97 ± 0.04	97.89 ± 0.02	10.05 ± 0.01	10.05 ± 0.01	10.04 ± 0.02
3	White, free-flowing powder	97.94 ± 0.01	97.96 ± 0.03	97.84 ± 0.02	10.05 ± 0.02	10.05 ± 0.01	10.03 ± 0.01
6	White, free-flowing powder	97.93 ± 0.03	97.94 ± 0.02	97.71 ± 0.16	10.04 ± 0.02	10.04 ± 0.01	10.02 ± 0.02

3.6 *In-vivo* pharmacokinetic study

A bioavailability study was conducted on rats. The established method calculated the testosterone undecanoate concentration after a single oral dosage (10 mg/kg). The test displayed adequate accuracy and precision for application in bioavailability studies using a one-step extraction and a brief run time. Figure 11 depicts the mean plasma concentration-time profiles of testosterone undecanoate after oral administration of the drug suspension and the optimal testosterone undecanoate-loaded proniosomal formulation. PK Solver was used to determine non-compartmental pharmacokinetic parameters, as displayed in Table 13.

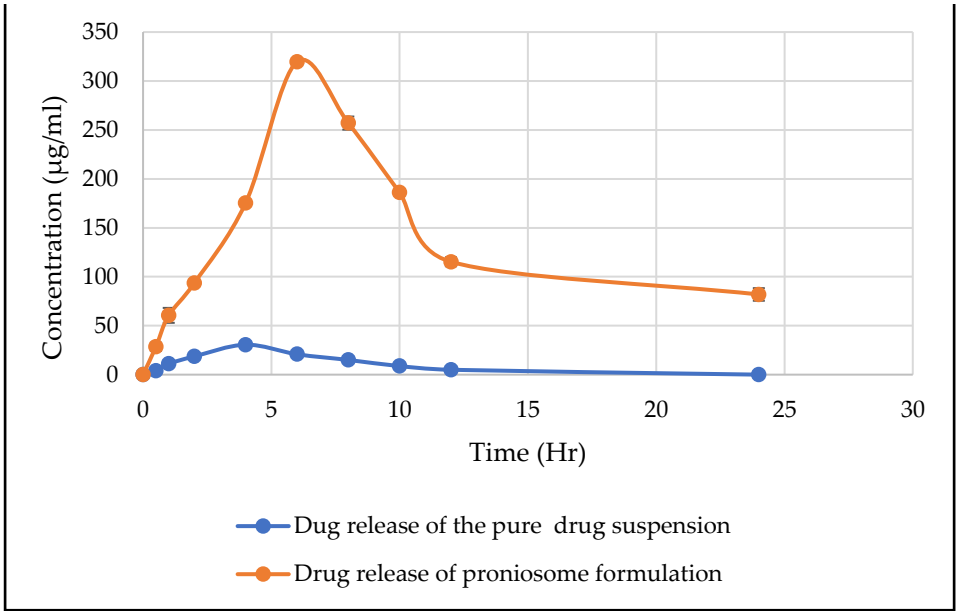

Figure 11. Mean plasma concentration-time curves of testosterone undecanoate after oral administration of its optimized proniosome formulation (equivalent to 10 mg/kg) and testosterone undecanoate drug suspension (10mg/kg) (mean ± SD, n = 3).

Table 13. Pharmacokinetic parameters

Parameter	Pharmacokinetic parameters	
	Pure drug suspension	Optimized proniosome formulations
$t_{1/2}$ (h)	3.279 ± 0.786	9.648 ± 0.591
Tmax (h)	4.000 ± 0.001	6.000 ± 0.001
Cmax (μg/ml)	31.378 ± 1.568	319.608 ± 3.441
AUC $_{0\text{-}24}$ (μg/ml*h)	192.551 ± 2.181	3374.956 ± 70.656
AUC $_{0\text{-}\infty}$.μg/ml*h)	219.259 ± 8.812	4518.856 ± 221.846
AUMC $_{0\text{-}\infty}$ (μg/ml*h²)	1490.273 ± 199.331	78354.149 ± 8163.846
MRT (h)	6.794 ± 0.675	17.310 ± 0.948
Vz/F ((mg/kg)/(μg/ml)	0.216 ± 0.046	0.031 ± 0.001
Cl/F ((mg/kg)/(μg/ml)/h)	0.046 ± 0.002	0.002 ± 0.001

The Cmax values of testosterone undecanoate from the pure drug suspension and its optimized proniosome formulations were found to be 31.378 ± 1.568 μg/ml and 319.608 ± 3.441μg/ml, respectively. Tmax for testosterone undecanoate in its optimized proniosome formulations and pure drug suspension was 4.0 hours and 6.0 hours, respectively. In the event of an optimized proniosomal formulation, other indices, such as $AUC_{0\text{-}24}$, $AUMC_{0\text{-}24}$, $t_{1/2}$, and MRT, were higher than in the case of pure drug suspension. However, the pharmacokinetic parameters of the testosterone undecanoate proniosome showed that the proniosome enhanced the concentrations of testosterone undecanoate in blood, delayed clearance, and displayed sustained release properties. All of these findings suggested that testosterone undecanoate proniosome formulations drugs might remain for a much more extended period than pure drugs *in vivo*.

4. Conclusions

Using different ratios of span 60 and cholesterol, testosterone undecanoate-loaded proniosomal formulations were successfully fabricated using a slurry technique and optimized employing the central composite design. Based on percentage drug entrapment (%), Vesicle size (nm), and PDI, the proniosomal formulation DTU-PNs14 containing a DoE-optimized cholesterol and span 60 ratio was chosen as the optimal formulation. The formulation DTU-PNs14 was deemed to be the most optimal formulation since it had the optimum particle size and PDI (282.33 ± 1.52 nm and 0.181 ± 0.003) and the significantly high & optimum entrapment efficiency (98.12 ± 1.03%). The Higuchi model best explained the release of testosterone undecanoate from the formulations of proniosomes. It was observed that there was no change of any kind, including the color of the proniosomes, up to 6 months of storage. The results of the percentage drug entrapment indicated no leakage of the drug during the stability study. The *in vivo* pharmacokinetic study also revealed favorable results indicating that testosterone undecanoate proniosome formulations drug might remain longer than a pure drug *in vivo*.

5. Acknowledgements

The authors thank and acknowledge the School of Pharmacy, Abhilashi University, Chail-Chowk, Mandi (H.P.) – 175028, India, for providing the research environment and laboratory support throughout the work.

Author Contributions: Conceptualization, A.S. and D.A.S.; methodology, C.K.; software, A.S.; validation, A.S., D.A.S. and C.K..; formal analysis, A.S.; investigation, A.S..; resources, A.S..; data curation, A.S..; writing—original draft preparation, A.S..; writing—review and editing, D.A.S.; visualization, D.A.S.; supervision, D.A.S.; project administration. All authors have read and agreed to the published version of the manuscript.

Funding: This research received no external funding.

Conflicts of Interest: The authors declare no conflict of interest.

References

[1] Saxena, A.; Apurvi, P.; Aslam, R. A Review on Proniosomes: A Propitious Outlook to the Provesicular Drug Delivery System. *Current drug delivery.* **2023,** *20*(8), 1115-1126. 10.2174/1567201820666221019093921.

[2] Mittal, S.; Chaudhary, A.; Chaudhary, A.; Kumar, A. Proniosomes: the effective and efficient drug-carrier system. *Therapeutic delivery.* **2020,** *11* (2), 125-137. 10.4155/tde-2019-0065.

[3] Sabale, V.; Charde, M.; Dumore, N.; Mahajan, U. Recent Developments in Proniosomal Transdermal Drug Delivery: An Overview. *Current drug delivery.* **2023,** *20*(6), 683-693. 10.2174/1567201819666220422153059.

[4] Adki, K. M.; Kulkarni, Y. A. Chemistry, pharmacokinetics, pharmacology and recent novel drug delivery systems of paeonol. *Life sciences.* **2020,** *250*, 117544. 10.1016/j.lfs.2020.117544.

[5] Limongi, T.; Susa, F.; Marini, M.; Allione, M.; Torre, B.; Pisano, R.; di Fabrizio, E. Lipid-Based Nanovesicular Drug Delivery Systems. *Nanomaterials (Basel, Switzerland).* **2021,** *11*(12). 10.3390/nano11123391.

[6] Zhu, Y.; Cao, S.; Huo, M.; van Hest, J. C. M.; Che, H. Recent advances in permeable polymersomes: fabrication, responsiveness, and applications. *Chemical science.* **2023,** *14*(27), 7411-7437. 10.1039/d3sc01707a.

[7] Abildgaard, J.; Petersen, J. H.; Bang, A. K.; Aksglaede, L.; Christiansen, P.; Juul, A.; Jørgensen, N. Long-term testosterone undecanoate treatment in the elderly testosterone deficient male: An observational cohort study. *Andrology.* **2022,** *10*(2), 322-332. 10.1111/andr.13124.

[8] An, J.; Kong, H. Comparative application of testosterone undecanoate and/or testosterone propionate in induction of benign prostatic hyperplasia in Wistar rats. *PloS one.* **2022,** *17*(5), e0268695. 10.1371/journal.pone.0268695.

[9] Chillarón, J. J.; Fernández-Miró, M.; Albareda, M.; Fontserè, S.; Colom, C.; Vila, L.; Pedro-Botet, J.; Flores Le-Roux, J. A. Testosterone undecanoate improves lipid profile in patients with type 1 diabetes and hypogonadotrophic hypogonadism. *Endocrine journal.* **2016,** *63*(9), 849-855. 10.1507/endocrj.EJ16-0195.

[10] Nieschlag, E.; Nieschlag, S. Testosterone deficiency: a historical perspective. *Asian journal of andrology.* **2014,** *16*(2), 161-8. 10.4103/1008-682x.122358.

[11] Saenger, P.; Steiner, M. Oral testosterone undecanoate is an effective treatment for micropenis therapy. *Pediatric investigation.* **2021,** *5*(4), 323-324. 10.1002/ped4.12304.

[12] Miller, J. A.; Nguyen, T. T.; Loeb, C.; Khera, M.; Yafi, F. A. Oral testosterone therapy: past, present, and future. *Sexual medicine reviews.* **2023,** *11*(2), 124-138. 10.1093/sxmrev/qead003.

[13] Swerdloff, R. S.; Dudley, R. E. A new oral testosterone undecanoate therapy comes of age for the treatment of hypogonadal men. *Therapeutic advances in urology.* **2020,** *12*, 1756287220937232. 10.1177/1756287220937232.

[14] Schlich, M.; Lai, F.; Maria Fadda, A.; Sinico, C.; Pini, E. Drug-Excipients Compatibility Studies in Proniosomal Formulation: A Case Study with Resveratrol. *Journal of nanoscience and nanotechnology.* **2021,** *21*(5), 2917-2921. 10.1166/jnn.2021.19056.

[15] Pankaj, S.; Rini, T.; Dandagi, P. Formulation and Evaluation of Proniosome Based Drug Delivery System of the Antifungal Drug Clotrimazole. *International Journal of Pharmaceutical Sciences and Nanotechnology.* **2013,** *6*, 1945-1951. 10.37285/ijpsn.2013.6.1.4.

[16] Radha, G. V.; Rani, T. S.; Sarvani, B. A review on proniosomal drug delivery system for targeted drug action. *Journal of basic and clinical pharmacy.* **2013,** *4*(2), 42-8. 10.4103/0976-0105.113609.

[17] Sudhamani, T.; Ganesan, V.; Priyadarsini, N.; Radhakrishnan, M. In *FORMULATION AND EVALUATION OF IBUPROFEN LOADED MALTODEXTRIN BASED PRONIOSOME*, **2010**.

[18] Cheriyan, P.; George, B. J.; Thomas, N.; Raj, P.; Samuel, J.; Carla, S. B. Formulation and characterization of maltodextrin based proniosomes of cephalosporins. *World Journal of Pharmaceutical Sciences.* **2015**, 62-74.

[19] Hsieh, C. M.; Yang, T. L.; Putri, A. D.; Chen, C. T. Application of Design of Experiments in the Development of Self-Microemulsifying Drug Delivery Systems. *Pharmaceuticals (Basel, Switzerland).* **2023,** *16*(2). 10.3390/ph16020283.

[20] Rampado, R.; Peer, D. Design of experiments in the optimization of nanoparticle-based drug delivery systems. *Journal of controlled release : official journal of the Controlled Release Society.* **2023,** *358*, 398-419. 10.1016/j.jconrel.2023.05.001.

[21] Mukerjee, A.; Vishwanatha, J. K. Formulation, characterization and evaluation of curcumin-loaded PLGA nanospheres for cancer therapy. *Anticancer research.* **2009,** *29*(10), 3867-3875.

[22] Maji, R.; Dey, N. S.; Satapathy, B. S.; Mukherjee, B.; Mondal, S. Preparation and characterization of Tamoxifen citrate loaded nanoparticles for breast cancer therapy. *International journal of nanomedicine.* **2014,** *9*, 3107.

[23] Cetin, M.; Atila, A.; Kadioglu, Y. Formulation and in vitro characterization of Eudragit® L100 and Eudragit® L100-PLGA nanoparticles containing diclofenac sodium. *AAPS PharmSciTech.* **2010,** *11*(3), 1250-6. 10.1208/s12249-010-9489-6.

[24] Jain, S. K.; Awasthi, A. M.; Jain, N. K.; Agrawal, G. P. Calcium silicate based microspheres of repaglinide for gastroretentive floating drug delivery: preparation and in vitro characterization. *Journal of controlled release : official journal of the Controlled Release Society.* **2005,** *107*(2), 300-9. 10.1016/j.jconrel.2005.06.007.

[25] Averineni, R. K.; Shavi, G. V.; Gurram, A. K.; Deshpande, P. B.; Arumugam, K.; Maliyakkal, N.; Meka, S. R. J. B. o. M. S. PLGA 50: 50 nanoparticles of paclitaxel: development, in vitro anti-tumor activity in BT-549 cells and in vivo evaluation. *Bull. Mater. Sci.* **2012,** *35*(3), 319-326.

[26] Dora, C. P.; Singh, S. K.; Kumar, S.; Datusalia, A. K.; Deep, A. Development and characterization of nanoparticles of glibenclamide by solvent displacement method. *Acta pol pharm.* **2010,** *67*(3), 283-290.

[27] Rasul, A.; Imran Khan, M.; Ur Rehman, M.; Abbas, G.; Aslam, N.; Ahmad, S.; Abbas, K.; Akhtar Shah, P.; Iqbal, M.; Ahmed Al Subari, A. M.; Shaheer, T.; Shah, S. In vitro Characterization and Release Studies of Combined Nonionic Surfactant-Based Vesicles for the Prolonged Delivery of an Immunosuppressant Model Drug. *International journal of nanomedicine.* **2020,** *15*, 7937-7949. 10.2147/ijn.S268846.

[28] Kumar, A.; Gulati, M.; Singh, S. K.; Gowthamarajan, K.; Prashar, R.; Mankotia, D.; Gupta, J. P.; Banerjee, M.; Sinha, S.; Awasthi, A.; Corrie, L.; Kumar, R.; Patni, P.; Kumar, B.; Pandey, N. K.; Sadotra, M.; Kumar, P.; Kumar, R.; Wadhwa, S.; Khursheed, R. Effect of co-administration of probiotics with guar gum, pectin and eudragit S100 based colon targeted mini tablets containing 5-Fluorouracil for site specific release. *Journal of Drug Delivery Science and Technology.* **2020,** *60*, 102004. 10.1016/j.jddst.2020.102004.

[29] Liu, H.; Tu, L.; Zhou, Y.; Dang, Z.; Wang, L.; Du, J.; Feng, J.; Hu, K. Improved Bioavailability and Antitumor Effect of Docetaxel by TPGS Modified Proniosomes: In Vitro and In Vivo Evaluations. *Scientific reports.* **2017,** *7*, 43372. 10.1038/srep43372.

[30] Nasr, M. In vitro and in vivo evaluation of proniosomes containing celecoxib for oral administration. *AAPS PharmSciTech.* **2010,** *11*(1), 85-9. 10.1208/s12249-009-9364-5.